Electronic Supplementary Material (ESI) for RSC Advances.

Supporting Information

Enhanced device performance and stability of perovskite solar cells with low-temperature ZnO/TiO_2 bilayered electron transport layers

Caifeng Zhang,[a,b] Guangmei Zhai,*[a,b] Yong Zhang,[a,b,c] Wenhui Gao,[a,b] Zhimeng Shao,[a,b] Lulu Zheng,[a,b] Fuhong Mei,[a,b] Hua Zhang,*[a,b] Yongzhen Yang,[a,b] Xuemin Li,[a,b] Xuguang Liu,[a,b, c] and Bingshe Xu[a,b]

a.Key Laboratory of Interface Science and Engineering in Advanced Materials of Ministry of Education, Research Centre of Advanced Materials Science and Technology, Taiyuan University of Technology, Taiyuan, Shanxi 030024, China.

E-mail: zhaiguangmei@tyut.edu.cn (G. Zhai); zhanghua01@tyut.edu.cn (H. Zhang)

b.CAS Key Laboratory of Renewable Energy，Guangzhou 510640, China

c.Collaborative Innovation Centre for Advanced Thin-film Optoelectronic Materials and Devices in Shanxi Province, Taiyuan, Shanxi 030024, China

d.College of Materials Science and Engineering, Taiyuan University of Technology, Taiyuan, Shanxi 030024, China

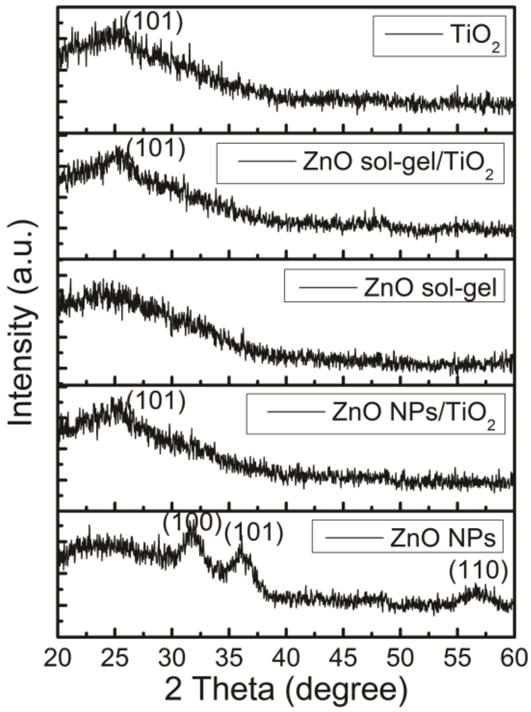

Fig. S1 Grazing Incidence X-ray diffraction (GIXRD) patterns of different electron transport layers deposited on glass.

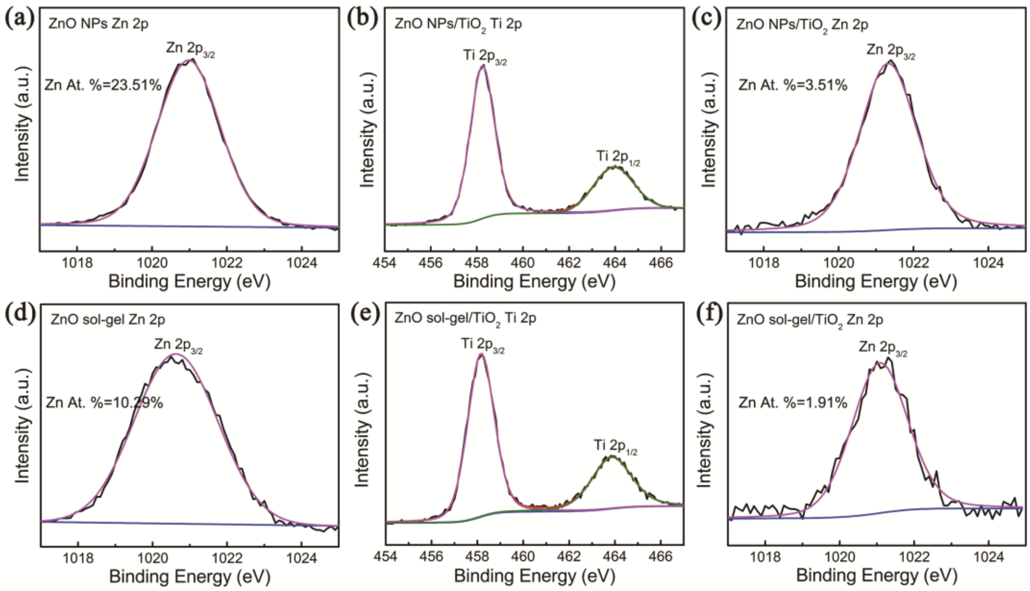

Fig. S2 Zn 2p and Ti 2p XPS spectra of (a) a ZnO NP-film, (b)(c)a ZnO NPs/TiO_2 bilayered film, (d) a ZnO sol-gel film, and (e) (f) a ZnO sol-gel/TiO_2 bilayered film. (Note: a small amount of Zn can be still detected on the surface of the ZnO/TiO_2 bilayer, indicating that TiO_2 does not completely cover the ZnO films probably due to the rough surface of FTO.)

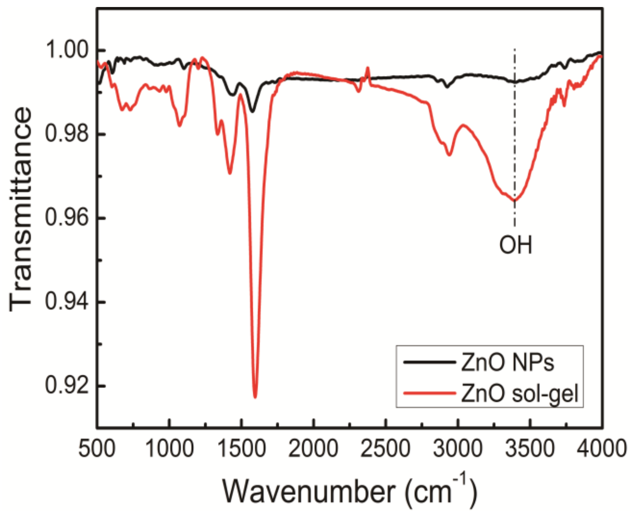

Fig. S3 FTIR spectra of a ZnO NP-film and a ZnO sol-gel film.

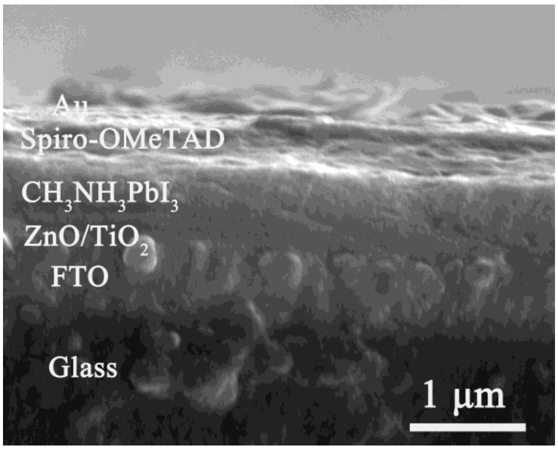

Fig. S4 The cross-sectional SEM image of a PSC device with the structure of glass/FTO/ ZnO/TiO_2 /$CH_3NH_3PbI_3$/Spiro-OMeTAD/Au.

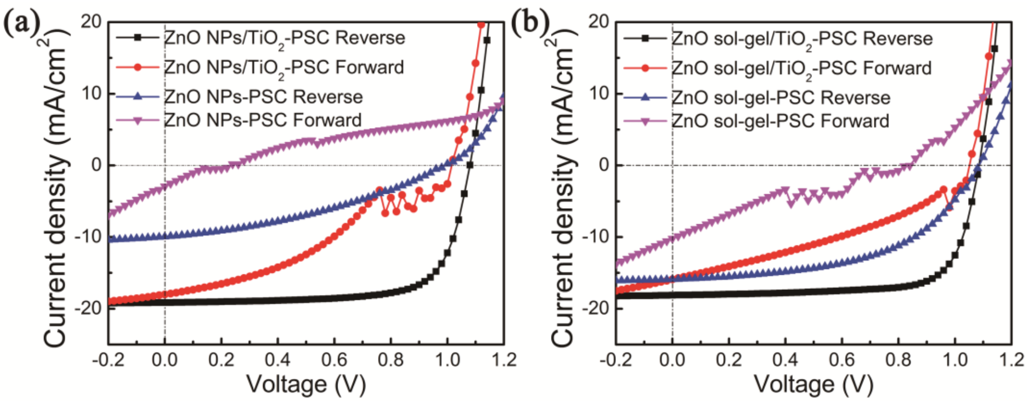

Fig. S5 J-V curves of perovskite solar cells fabricated (a) on a ZnO NP-film and a ZnO NPs/TiO_2 bilayered film; (b) on a ZnO sol-gel film and a ZnO sol-gel/TiO_2 bilayered film under reverse and forward scans.

Table S1 Photovoltaic parameters of different devices under reverse and forward scans.

	V_{oc} (V)	J_{sc} (mA/cm^2)	FF (%)	PCE (%)
ZnO NPs-PSC Reverse	0.98	9.94	36.50	3.56
ZnO NPs-PSC Forward	0.22	2.91	17.84	0.11
ZnO NPs/TiO_2-PSC Reverse	1.06	19.14	73.89	15.0
ZnO NPs/TiO_2-PSC Forward	1.00	18.01	34.65	6.24
ZnO sol-gel-PSC Reverse	1.08	15.90	52.58	9.03
ZnO sol-gel-PSC Forward	0.84	10.23	27.73	2.38
ZnO sol-gel/TiO_2-PSC Reverse	1.08	18.11	74.38	14.55
ZnO sol-gel/TiO_2-PSC Forward	1.04	15.91	36.29	6.01

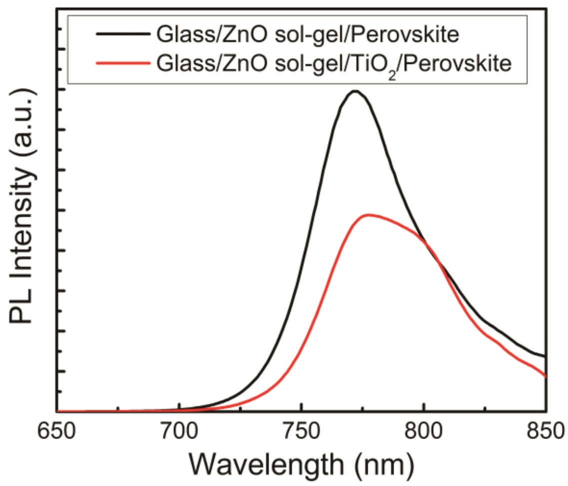

Fig. S6 The steady-state photoluminescence spectra of perovskite films deposited on a ZnO sol-gel film and a ZnO sol-gel/TiO_2 bilayer film.

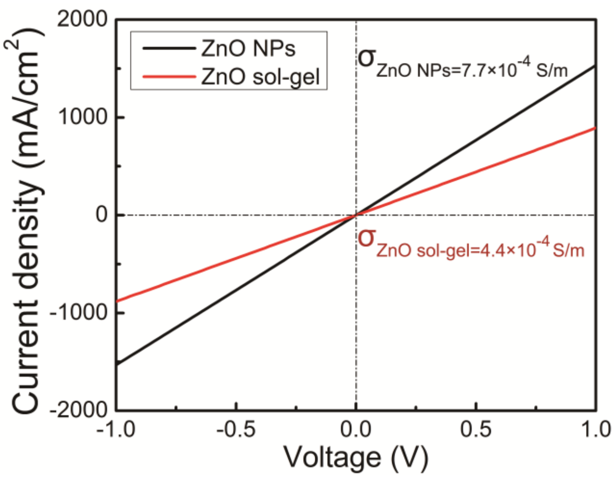

Fig. S7 J-V curves of the ZnO-NP and ZnO sol-gel films with the device structure of ITO/ZnO/Au in dark.

Conductivity measurement: In order to obtain electrical conductivities of the ZnO NP-film and ZnO sol-gel film, we meausured *J-V* curves of devices with the structure of ITO/ZnO/Au. The obtained *J-V* curves are shown in Fig. S7 in the supporting information. Their conductivities were further calculated out via the following formula.

$$\sigma = \frac{l}{RS}$$

where σ is conductivity (S/m), *l* film thickness (m), *R* film resistance (Ω), and *S* film area (m^2).

The calculated conductivities of the ZnO NP-film and ZnO sol-gel film are 7.7×10^{-4} S/m and 4.4×10^{-4} S/m, respectively.

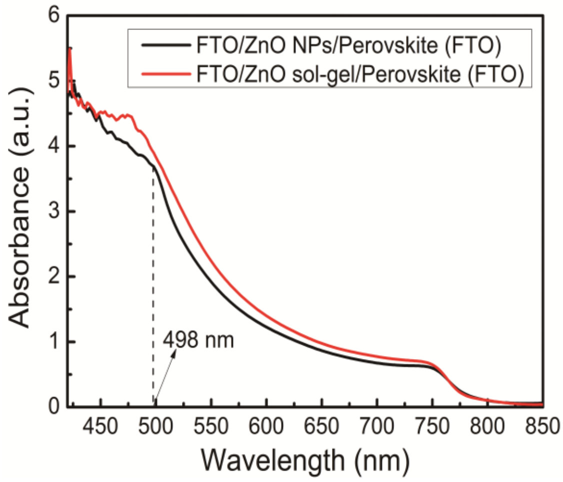

Fig. S8 Absorbance spectra of perovskite films deposited on a ZnO NP-film and a ZnO sol-gel film.

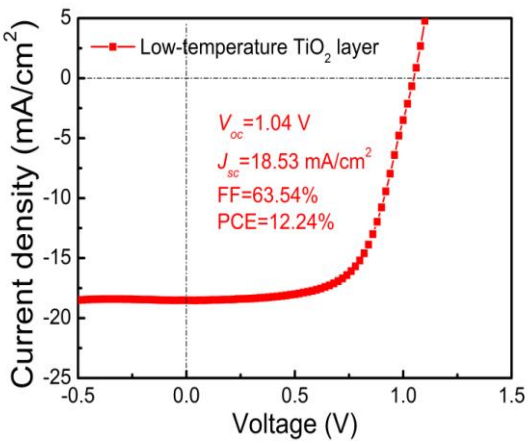

Fig. S9 Typical *J-V* curve of the perovskite solar cell based on a low-temperature TiO_2 electron transport layer.